

# Nanoscale

Accepted Manuscript



This is an *Accepted Manuscript*, which has been through the Royal Society of Chemistry peer review process and has been accepted for publication.

*Accepted Manuscripts* are published online shortly after acceptance, before technical editing, formatting and proof reading. Using this free service, authors can make their results available to the community, in citable form, before we publish the edited article. We will replace this *Accepted Manuscript* with the edited and formatted *Advance Article* as soon as it is available.

You can find more information about *Accepted Manuscripts* in the [Information for Authors](#).

Please note that technical editing may introduce minor changes to the text and/or graphics, which may alter content. The journal's standard [Terms & Conditions](#) and the [Ethical guidelines](#) still apply. In no event shall the Royal Society of Chemistry be held responsible for any errors or omissions in this *Accepted Manuscript* or any consequences arising from the use of any information it contains.



Journal Name

ARTICLE

# Transformation of self-assembly of a TTF Derivative at 1-phenyloctane/HOPG Interface Studied by STM— from Nanoporous Network to Linear Structure

Jing Xu,<sup>a</sup> Xunwen Xiao,<sup>b</sup> Ke Deng,<sup>\*a</sup> and Qingdao Zeng<sup>\*a</sup>Received 00th January 20xx,  
20xx,

The self-assembly of a tetrathiafulvalene (TTF) derivative (EDTTF) and 1,3,5-tris (10-Carboxydecyloxy)-benzene (TCDB) heterobilayer nanostructure at 1-phenyloctane/HOPG interface under ambient conditions has been studied by scanning tunneling microscopy (STM). EDTTF and TCDB could co-assemble into a brand new hexagonal network with one of the largest nano-cavities. Finally, the nanoporous network would transform into the more stable linear structure. Density functional theory (DFT) calculations have been performed to reveal the formation mechanism.

Accepted 00th January 20xx

DOI: 10.1039/x0xx00000x

[www.rsc.org/](http://www.rsc.org/)

## Introduction

Tetrathiafulvalene (TTF) and its derivatives have been extensively studied in the development of molecular electronics due to their high electrical conductivity, strong electron-donating abilities and excellent redox properties<sup>1-3</sup>. With sulphur atoms in the core part, TTF derivatives exhibit high symmetry, planarity and reversible redox features, which are beneficial in electronics<sup>1-3</sup>.

Since most electronic devices have to be supported by a conductive substrate, the orientation, conformation, packing patterns, and structural defects of the interfacial region can be of great importance. They may affect the rate of carrier mobility and even change the way of carrier transportation. Among various technical methods, scanning tunnelling microscopy (STM) has absolute advantages in reflecting the position and distribution of molecules on 2D surfaces or interfaces with resolution at atomic level<sup>4-7</sup>.

Previously, STM has been employed to study self-assembled structures of some TTF derivatives. For example, Chun-hsien

Chen studied template-assisted self-assembly of alkyl-derivatized TTF<sup>8</sup>. Simon Laurent et al. studied the influence of deposition mode on the assembly of TTF derivatives<sup>9</sup>. Steven De Feyter et al. studied self-assembled structures of a series of TTF derivatives with different functional groups and alkyl chains of various number and lengths<sup>10, 11</sup>. These studies all mentioned solvent effects in the experiments. Moreover, the target TTF systems chosen in these studies were all TTF derivatives with long alkyl chains. In the work of Steven De Feyter et al., they reported self-assemblies of three TTF derivatives without long alkyl chains. The results showed that STM images could not be obtained at 1-phenyloctane/graphite interface<sup>11</sup>. It should be noted that TTF derivatives without long alkyl chains have rarely been reported.

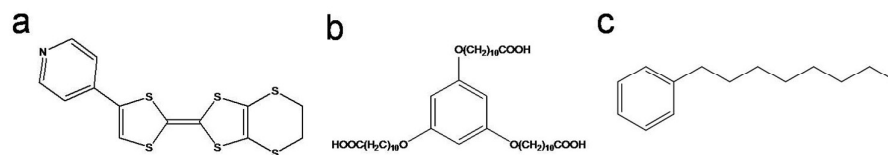
In this study, 4-pyridyl-(ethylenedithio) TTF, a pyridyl-substituted TTF derivative (EDTTF, Scheme 1a) without alkyl chains was selected to study its self-assembled structure by STM. Previous studies showed that a novel proton-electron coupled system based on N<sup>+</sup>-H•••N hydrogen-bonding in the bulk phase was observed<sup>12</sup>. However, our results showed that EDTTF itself could not assemble into orderly network at 1-phenyloctane/HOPG interface under STM. Therefore, we introduced the 1,3,5-tris(10-Carboxydecyloxy)-benzene (TCDB, Scheme 1b) molecule into our target system.

EDTTF and TCDB could co-assemble into a brand new hexagonal network. This network with one of the largest nano-cavities was detected by STM at 1-phenyloctane/HOPG interface<sup>13</sup>. Finally, this metaphase pattern would transform into linear closely packed pattern. Density functional theory (DFT) calculations have been performed to reveal the formation mechanism.

<sup>a</sup> Key Laboratory of Standardization and Measurement for Nanotechnology, National Center for Nanoscience and Technology (NCNST), 11 ZhongguancunBeiyitiao, Beijing 100190, P. R. China. E-mail: [zengqd@nanocr.cn](mailto:zengqd@nanocr.cn), [kdeng@nanocr.cn](mailto:kdeng@nanocr.cn)

<sup>b</sup> College of Chemical Engineering, Ningbo University of Technology, Ningbo 315211, P. R. China. E-mail: [xunwenxiao@nbut.edu.cn](mailto:xunwenxiao@nbut.edu.cn)

† Electronic Supplementary Information (ESI) available: [details of any supplementary information available should be included here]. See DOI: 10.1039/x0xx00000x



**Scheme 1.** Chemical structures of EDTTF (a), TCDB (b) and 1-phenyloctane (PO, c)

## Results and discussion

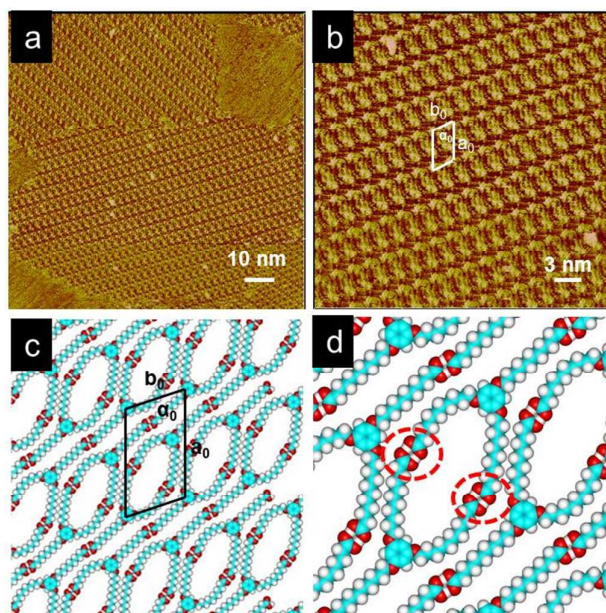


**Figure 1.** (a) Large scale STM image of TCDB self-assembly on the HOPG surface.  $I_{\text{set}} = 299.1$  pA;  $V_{\text{bias}} = 599.1$  mV; (b) High-resolution STM image of TCDB on the HOPG surface.  $I_{\text{set}} = 289.9$  pA;  $V_{\text{bias}} = 599.1$  mV; (c) and (d) are calculated molecular models for the observed area in (a).

The solvent used in the experiments was 1-phenyloctane (PO, Scheme 1c). A droplet of solution containing TCDB was dropped onto the freshly cleaved HOPG to form the stable monolayer nano-template. Typically, TCDB molecules can form a molecular template with well-defined rectangular nanopores at 1-phenyloctane/HOPG interface in a large scale. Figure 1a shows the large-scale STM image of assembly of TCDB. Detailed assembly structures are shown in Figure 1b. It could be noted that each tetragonal cavity is formed by two TCDB molecules. Careful analysis reveals that two TCDB molecules form two pairs of hydrogen bonds via the terminal carboxylic groups (see the red dashed circles in Figure 1d). Figure 1c is the corresponding molecular model calculated by DFT method on the basis of STM observations. The measured unit cell is superimposed on the molecular model with  $a_0 = 3.9 \pm 0.1$  nm,  $b_0 = 2.2 \pm 0.1$  nm,  $\alpha_0 = 73 \pm 2^\circ$ .

Obviously, this type of network is large enough to be used as a template to accommodate various functional molecules as guest species. Previous studies have reported the co-adsorption of guest molecules, such as coronene, phthalocyanine and other functional macrocycles into these nanopores<sup>14-16</sup>. After TCDB template with rectangular nanopores was formed, a droplet of EDTTF solution was applied onto the TCDB self-assembly structure. Figure 2a shows a large scale STM image of TCDB/EDTTF system. Two kinds of patterns coexist (denoted as domain I, II). Domain I is the traditional pure TCDB assembly. While in domain II, a new hexagonal network appears. Interestingly, EDTTF molecules did not fill in the nanopores of TCDB template as we had expected. Instead, a totally different hexagonal network constructed by bright points was observed. We denoted this hexagonal network as EDTTF-Loose pattern (Figure 2a, right part). Figure 2b shows the high resolution STM image of EDTTF-Loose pattern. In the hexagonal network, each edge was covered with two bright rectangle points, and each vertex was surrounded with three bright points. Some defects with missing bright points, which are indicated by the yellow arrows in Figure 2b, can be visualized in the STM image. The length of each bright point is approximately 1.5 nm ( $L_1$ , Figure 2b), which is in accordance with the size of one EDTTF molecule. We deduced that each bright point corresponded to one EDTTF molecule. The length of the edge of hexagonal network is approximately 3.4 nm, which is nearly twice the length of an alkyl chain of TCDB. We suggested that in the

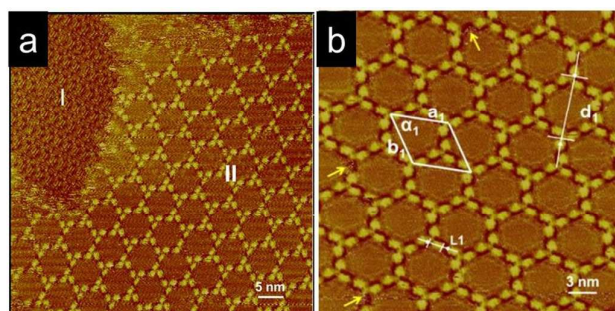


**Figure 2.** (a) Coexistence of traditional TCDB self-assembly (I) and EDTTF-Loose pattern (II). Tunneling condition:  $I_{\text{set}}=299.1$  pA,  $V_{\text{bias}}=599.1$  mV. (b) High-resolution STM image of EDTTF-Loose pattern. Tunneling condition:  $I_{\text{set}}=349.1$  pA,  $V_{\text{bias}}=599.1$  mV. The distance of  $d_1=7.0 \pm 0.1$  nm,  $L_1=1.5 \pm 0.1$  nm. The yellow arrows point out the missing bright points in EDTTF-Loose pattern. A unit cell was superimposed on EDTTF-Loose pattern with the corresponding parameters shown in Table 1.

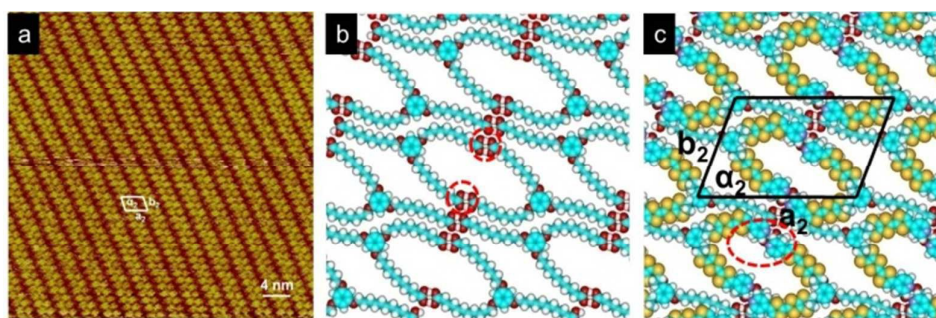


**Figure 3.** (a) STM image of EDTTF-Tight pattern. Tunneling condition:  $I_{\text{set}}=349.1\text{pA}$ ,  $V_{\text{bias}}=599.1\text{mV}$ . Calculated molecular models of (b) optimized TCDB2 pattern and (c) TCDB2-EDTTF. A unit cell was superimposed on (a) and (c) separately with parameters shown in Table 1.

TCDB/EDTTF system, the three alkyl chains of TCDB were fully extended, and TCDB molecules underwent symmetry transformation from original  $C_5$  symmetry to  $C_3$  symmetry. Then, every TCDB molecule could interact with three TCDB molecules via hydrogen bonding through the terminal carboxylic groups (Figure S3). Accordingly, a hexagonal network could be formed. Considering that EDTTF itself could not be stably adsorbed on the graphite, EDTTF would only deposit on the alkyl chains of the TCDB frame. A cross-sectional profile (Figure S1) corresponding to Figure 2a shows that the height of the bright spots is higher than that of the traditional TCDB network. Therefore, we could infer the bright spots represented EDTTF molecules due to the height as well as the strong electronic density of the core part of EDTTF. To obtain the size of the hexagonal cavity, we measured the distance between the two opposite vertexes ( $d_1$ , Figure 2b). The distance  $d_1$  is  $7.0 \pm 0.1$  nm, which means that the network is with one of the largest hexagonal cavities ever observed by STM. The measured unit cell is superimposed on the molecular model with  $a_1 = 6.1 \pm 0.1$  nm,  $b_1 = 6.1 \pm 0.1$  nm and  $\alpha_1 = 59 \pm 2^\circ$  (Figure 2b).

After obtaining the hexagonal nanostructure, the sample was kept for 48 hours and detected by STM again. Surprisingly, the hexagonal EDTTF-Loose pattern disappeared and was replaced by a compacted linear pattern (EDTTF-Tight pattern, Figure 3a). In Figure 3a, lamellae structure constructed by bright points could be observed. The bright points staggered alternately in each line. As we know, EDTTF deposited on the alkyl chains. Thus, the dramatic changes of the arrangement of EDTTF indicated that the hexagonal TCDB frame gradually transformed back to the closely-packing frame. In this process, the traditional TCDB packing pattern was also optimized to adapt to the illustrative molecular model (denoted by TCDB2 pattern, Figure 3b). The red dash circle in Figure 3b marked out the hydrogen bonds between TCDB molecules via the terminal carboxylic groups. Furthermore, hydrogen bonding ( $\text{C-H} \cdots \text{N}$ ) is formed between the two pyridine rings of the EDTTF dimer deposited on the TCDB alkyl chains (marked by the red dash circle in Figure 3c), which contributes about  $-14.322$  kcal  $\text{mol}^{-1}$  to the total energy. The measured unit cell is superimposed on the molecular model with  $a_2 = 3.5 \pm 0.1$  nm,  $b_2 = 2.2 \pm 0.1$  nm and  $\alpha_2 = 69 \pm 2^\circ$  (Figure 3c).

Although the pure TCDB cavities could resize to accommodate guest molecules according to previous reports<sup>6,15</sup>, how could the hexagonal structure be constructed with EDTTF molecules immobilized on the edge? To answer this question, density functional theory (DFT) calculation was performed to understand the formation mechanism based on the observed phenomena. The calculated lattice parameters for 2D networks are summarized in Table 1. The calculated parameters agree well with the experimental data. The cell size, the structures, and the geometry of the adsorbates are presented in the supporting information (Figure S4). In the surface assembly system, the interaction between adsorbates and substrate plays an important role. Therefore, we presented the total energy (including the interaction energy between adsorbates and the interaction energy between adsorbates and substrate) in Table 2. Furthermore, a reasonable way to compare the thermodynamic stability of the different arrays should be the total energy per unit area. Then we also presented the total energy per unit area of the system in Table 2.

Firstly, we calculated the total energy per unit area of the assembled structure of pure packing TCDB ( $-0.286$  kcal  $\text{mol}^{-1} \text{ \AA}^{-2}$ ). Since pure TCDB assembly was a well-known packing pattern, before the EDTTF molecules were introduced into the system, this value can be viewed as a reference. Then, we proposed the hexagonal pattern of TCDB framework (TCDB1) with EDTTF deposited on the alkyl chains (denoted by TCDB1-EDTTF, Figure 4a). The total energy per unit area of the hexagonal TCDB (TCDB1) is only  $-0.077$  kcal  $\text{mol}^{-1} \text{ \AA}^{-2}$ , which is much higher than that of the pure TCDB packing pattern. This is why we could not observe the pure hexagonal pattern of TCDB framework. Then we calculated the total energy per unit area of TCDB1-EDTTF, in this model EDTTF directly deposited on the alkyl branches of the hexagonal TCDB framework. However, the total energy per unit area of TCDB1-EDTTF is only  $-0.158$  kcal  $\text{mol}^{-1} \text{ \AA}^{-2}$ , which is less stable than that of the pure packing TCDB assembly. It means that this model was not an energetically favourable structure. Therefore, we considered the solvent effect, and proposed a TCDB1-EDTTF-PO model (Figure 4b), in which the solvents (1-phenyloctane, PO) were conjectured to participate into the TCDB1/EDTTF system. Figure 4c and Figure 4d show the details of the

molecular models, respectively. Hydrogen bonding (C-H  $\cdots$  N) also exists among the three pyridine rings at the end of the

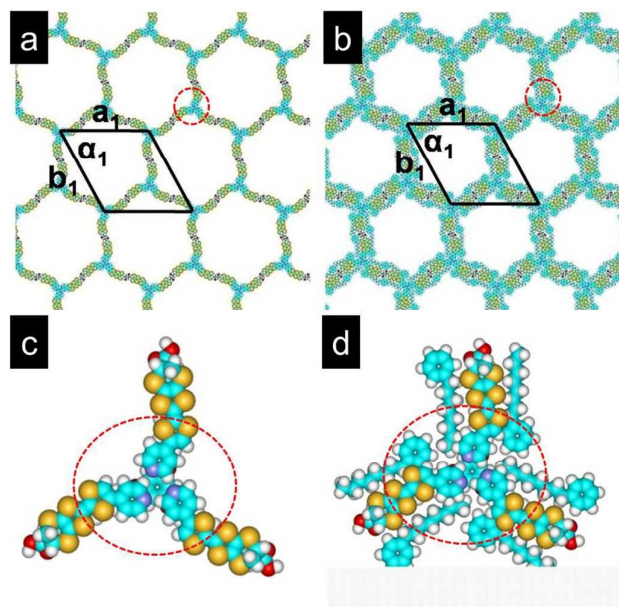


**Figure 4.** Calculated molecular models of (a) TCDB1-EDTTF and (b) TCDB1-EDTTF-PO. (c) and (d) show the details of the red dash circles of (a) and (b), respectively.

EDTTF molecules (marked by the red dash circle in Figure 4), which helps the three donors together in the hexagonal phase. Careful calculations show that the interaction energy of hydrogen bonding is about  $-23.237 \text{ kcal mol}^{-1}$ .

It is worth pointing out that the length of 1-phenyloctane (PO) is approximately 1.7 nm, which matches well to the length of the alkyl chain of TCDB. With the matching size, in presence of the strong interaction between PO and substrate, PO adsorbed on the graphite could interact with the alkyl chain side-by-side. Two PO molecules located beside an alkyl chain. The total energy per unit area of TCDB1-EDTTF-PO is  $-0.297 \text{ kcal mol}^{-1} \text{ \AA}^{-2}$ , and a little less than that of pure TCDB system ( $-0.286 \text{ kcal mol}^{-1} \text{ \AA}^{-2}$ ). Evidently, the participation of PO strengthens the

**Table 1.** Experimental (Expt.) and Calculated (Cal.) lattice parameters for TCDB, EDTTF-Loose and EDTTF-Tight pattern.

		Unit cell parameters		
		a (nm)	b (nm)	$\alpha$ ( $^\circ$ )
TCDB	Expt.	$3.9 \pm 0.1$	$2.2 \pm 0.1$	$73 \pm 2$
	Cal.	3.80	2.25	73.00
EDTTF-Loose	Expt.	$6.1 \pm 0.1$	$6.1 \pm 0.1$	$59 \pm 2$
	Cal.	6.08	6.08	60.00
EDTTF-Tight	Expt.	$3.5 \pm 0.1$	$2.2 \pm 0.1$	$69 \pm 2$
	Cal.	3.59	2.28	69.00

stability of the TCDB1/EDTTF system, and results in a more stable system comparing to the pure TCDB system. This is why when we introduced EDTTF, with PO as the solvent, we observed the hexagonal network. In addition, the total energy per unit area of TCDB1-EDTTF-PO is nearly equal to that of the pure TCDB network. Thus, the coexistence of TCDB and EDTTF-Loose pattern was observed in Figure 2a. It is notable that the total energy per unit area of TCDB2-EDTTF-Tight is the lowest ( $-0.529 \text{ kcal mol}^{-1} \text{ \AA}^{-2}$ ), indicating that EDTTF-Tight pattern is the most energetically favourable pattern.

Control experiments have been carried out to ensure that 1-phenyloctane takes part in the TCDB/EDTTF system. We introduced another solvent octanoic acid (OA) as the counterpart into TCDB/EDTTF system. However, we could only observe the final EDTTF-Tight pattern instead of the hexagonal network (Figure S2). We noticed that the length of PO is about 1.7 nm, while the length of OA is 1.1 nm. It means that due to the mismatch of the length between the solvent OA and the alkyl chain, the test solvent OA could not participate in the TCDB/EDTTF system. The control experiments proved our conjecture that the hexagonal network appeared really because of the participation of 1-phenyloctane in the TCDB/EDTTF system.

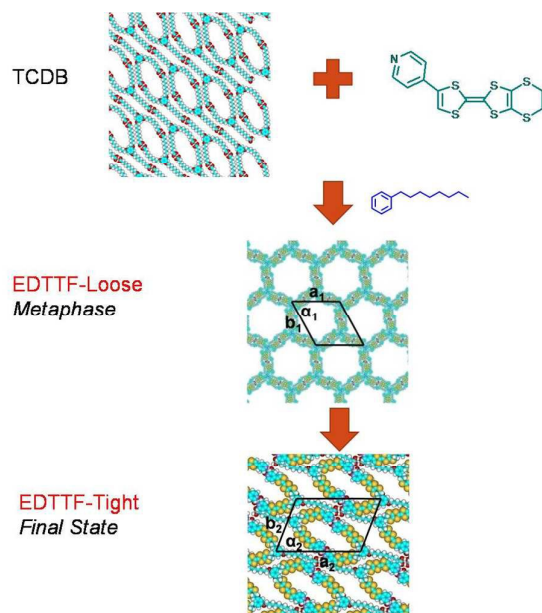
It is interesting to investigate why EDTTF preferentially adsorbed on top of the alkyl chains of TCDB. As mentioned before, EDTTF itself could not assemble into orderly network at 1-phenyloctane/HOPG interface under STM. It means that without external fixation, EDTTF could not be stably recorded by STM observation. In our study, TCDB molecules can form a molecular template with well-defined rectangular nanopores in a large scale. Thus, the alkyl chains should be considered not only as the "substrate" to support

**Table 2.** Total Energy and Energy per Unit Area for EDTTF-Loose and EDTTF-Tight pattern. Here, the more negative energy means the system is more stable.

		Interactions between molecules ( $\text{kcal mol}^{-1}$ )	Interactions between molecules and substrate ( $\text{kcal mol}^{-1}$ )	Total energy ( $\text{kcal mol}^{-1}$ )	Energy per unit area ( $\text{kcal mol}^{-1} \text{ \AA}^{-2}$ )
TCDB		-67.137	-166.817	-233.954	-0.286
EDTTF-Loose	TCDB1	-76.266	-167.280	-243.546	-0.077
	TCDB1-EDTTF	-309.963	-196.342	-506.305	-0.158
	TCDB1-EDTTF-PO	-479.840	-470.971	-950.811	-0.297
EDTTF-Tight	TCDB2	-60.137	-165.817	-225.954	-0.296
	TCDB2-EDTTF	-233.148	-170.824	-403.972	-0.529

EDTTF, but also as a kind of external fixation to bind them tightly. In the above discussions, further analyses show that EDTTF molecules deposited on the alkyl chains could form hydrogen bonding (C-H  $\cdots$  N) between the pyridine rings both in the EDTTF-Loose pattern and EDTTF-Tight pattern. Obviously, the hydrogen bonding helps EDTTF stably deposit on the alkyl chains. We have calculated the energy between EDTTF and TCDB "substrate". For the EDTTF-Loose pattern, the energy between EDTTF and TCDB/PO "substrate" is more stable ( $-15.862 \text{ kcal mol}^{-1}$ ) than that between EDTTF and HOPG. For the EDTTF-Tight pattern, the energy between EDTTF and TCDB "substrate" is more stable ( $-8.955 \text{ kcal mol}^{-1}$ ) than that between EDTTF and HOPG. Therefore, EDTTF molecules prefer depositing on the alkyl chains rather than HOPG.

At last, we presented a scheme (Scheme 2) to illustrate the whole experimental process. Firstly, TCDB formed the close-packing pattern. When the EDTTF/1-phenyloctane solution were introduced into the system, the traditional TCDB pattern was likely to re-assemble into the hexagonal pattern with EDTTF deposited on the alkyl chains and 1-phenyloctane (PO) adsorbed on the graphite side-by-side near the alkyl chains. In this stage, TCDB pattern and EDTTF-Loose pattern could coexist. However, EDTTF-Loose pattern is still a metaphase state. Gradually, with overcoming the steric hindrance under the tension force and the movements of the solution molecules, the EDTTF-Loose pattern transformed to EDTTF-Tight pattern (the most energetically favourable pattern). EDTTF-Tight pattern should be the final state with absolute advantages in thermodynamics.



**Scheme 2.** Mechanism for the co-assembly of EDTTF and TCDB.

## Conclusion

In summary, an EDTTF molecule without long alkyl chains was successfully detected by STM for the first time at 1-phenyloctane/HOPG interface after introduction of TCDB molecules. Instead of being immobilized into the TCDB cavities, EDTTF deposited on the alkyl chains of TCDB molecules to form a heterobilayer hexagonal network under 1-phenyloctane solution. Such network was with one of the largest sizes ever observed by STM. DFT calculations helped to explain the mechanism and obtained the most reasonable molecular model. Finally, the metaphase EDTTF-Loose pattern would transform into the closely packed EDTTF-Tight pattern. High-resolution STM images, as well as DFT calculations, provide a new perspective to study the two-dimensional nanostructures at submolecular level. The experiment results promote our understanding of TCDB packing pattern in an indirect way. Moreover, the new sights may enhance the understanding of the self-assembly of EDTTF at interfaces and improve further applications in other EDTTF systems and the design of nanodevices.

## Experimental

### Sample preparation

The solvent used in this work was 1-phenyloctane (Aldrich) without further purification. A pyridyl-substituted TTF derivative, 4-pyridyl-(ethylenedithio)TTF (EDTTF, Scheme 1a) was synthesized according to previous report<sup>17</sup>. EDTTF and 1,3,5-tris(10-Carboxydecyloxy)-benzene (TCDB, Scheme 1b) were dissolved in 1-phenyloctane separately with concentration less than  $1.0 \times 10^{-4} \text{ M}$ . A piece of highly oriented pyrolytic graphite (HOPG, grade ZYB, NTMDT, Russia) substrate was freshly cleaved using adhesive tape. First, a droplet of solution containing TCDB was deposited on HOPG substrate and detected by STM. After traditional TCDB network with rectangular pores was observed, a droplet of EDTTF was dropped onto the TCDB molecular template and studied by STM. Then the sample was kept for 48 hours, during which solution would be added to maintain the liquid/solid environment. After the treatments, the sample was detected by STM again. All the samples were studied by STM with its tips immersed directly into the droplet.

### STM investigation

All STM experiments were performed with a NanoscopeIIIa scanning probe microscope system (Bruker, USA) in constant current mode under ambient conditions. STM tips were prepared by mechanically cutting of Pt/Ir wire (80/20). All the STM images provided are raw data and were calibrated by referring the underlying graphite lattice. Detailed tunneling conditions were given in the corresponding figure captions.

**Computational details**

Theoretical calculations were performed using DFT provided by DMol3 code<sup>18</sup>. We used the periodic boundary conditions (PBC) to describe the 2D periodic structure on the graphite in this work. The Perdew and Wang parameterization<sup>19</sup> of the local exchange correlation energy was applied in local spin density approximation (LSDA) to describe exchange and correlation. All-electron spin-unrestricted Kohn–Sham wave functions were expanded in a local atomic orbital basis. For the large system, the numerical basis set was applied. All calculations were all-electron ones, and performed with the medium mesh. Self-consistent field procedure was done with a convergence criterion of  $10^{-5}$  au on the energy and electron density. Combined with the experimental data, we have optimized the unit cell parameters and the geometry of the adsorbates in the unit cell. When the energy and density convergence criterion are reached, we could obtain the optimized parameters and the interaction energy between adsorbates.

To evaluate the interaction between the adsorbates and HOPG, we design the model system. In our work, adsorbates consist of  $\pi$ -conjugated benzene-ring. Since adsorption of benzene on graphite and graphene should be very similar, we have performed our calculations on infinite graphene monolayers using PBC. In the superlattice, graphene layers were separated by 40 Å in the normal direction and represented by orthorhombic unit cells containing two carbon atoms. When modeling the adsorbates on graphene, we used grapheme super cells and sampled the Brillouin zone by a  $1 \times 1 \times 1$  k-point mesh. The interaction energy  $E_{\text{inter}}$  of adsorbates with graphite is given by  $E_{\text{inter}} = E_{\text{tot(adsorbates/graphene)}} - E_{\text{tot(isolated adsorbates in vacuum)}} - E_{\text{tot(graphene)}}$ .

**Acknowledgements**

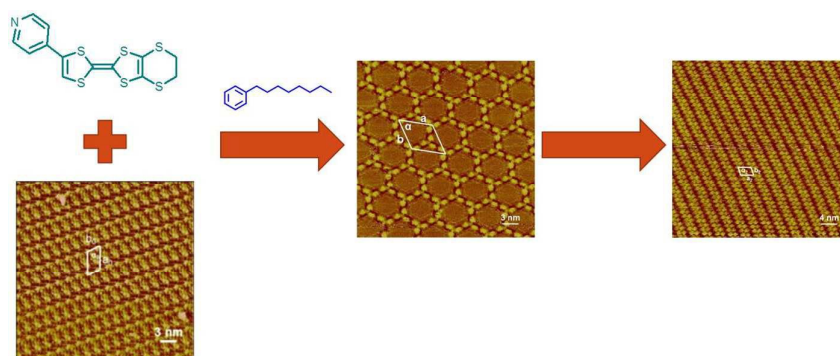
This work was supported by the National Basic Research Program of China (Nos. 2011CB932303, 2013CB934203, 2012CB933001) and the Chinese Academy of Sciences (Nos. YZ201318). The National Natural Science Foundation of China (Nos. 21472029, 51173031, 91127043 and 21372136) is also gratefully acknowledged.

**Notes and references**

1. F. Wudl, D. Wobschall and E. J. Hufnagel, *J. Am. Chem. Soc.*, 1972, **94**, 670-672.
2. J. Ferraris, D. O. Cowan, V. Walatka and J. H. Perlstein, *J. Am. Chem. Soc.*, 1973, **95**, 948-949.
3. M. Bendikov, F. Wudl and D. F. Perepichka, *Chem. Rev.*, 2004, **104**, 4891-4946.
4. S. De Feyter and F. C. De Schryver, *Chem. Soc. Rev.*, 2003, **32**, 139-150.
5. Y. Yang and C. Wang, *Chem. Soc. Rev.*, 2009, **38**, 2576-2589.

6. Y. T. Shen, L. Guan, X. Y. Zhu, Q. D. Zeng and C. Wang, *J. Am. Chem. Soc.*, 2009, **131**, 6174-6180.
7. J. Xu and Q. D. Zeng, *Curr. Org. Chem.*, 2014, **18**, 407-415.
8. S. L. Lee, Y. C. Chu, H. J. Wu and C. h. Chen, *Langmuir*, 2012, **28**, 382-388.
9. M. N. Nair, C. Mattioli, M. Cranney, J.-P. Malval, F. Vonau, D. Aubel, J.-L. Bubendorff, A. Gourdon and L. Simon, *J. Phys. Chem. C* 2015, **119**, 9334-9341.
10. M. M. S. Abdel Mottaleb, E. Gomar Nadal, S. De Feyter, M. Zdanowska, J. Veciana, C. Rovira, D. B. Amabilino and F. C. De Schryver, *Nano Lett.*, 2003, **3**, 1375-1378.
11. M. M. S. Abdel Mottaleb, E. Gomar Nadal, M. Surin, H. Uji-i, W. Mamdouh, J. Veciana, V. Lemaure, C. Rovira, J. Cornil, R. Lazzaroni, D. B. Amabilino, S. De Feyter and F. C. De Schryver, *J. Mater. Chem.*, 2005, **15**, 4601-4615.
12. S. C. Lee, A. Ueda, H. Kamo, K. Takahashi, M. Uruichi, K. Yamamoto, K. Yakushi, A. Nakao, R. Kumai, K. Kobayashi, H. Nakao, Y. Murakami and H. Mori, *Chem. Commun.*, 2012, **48**, 8673-8675.
13. K. Tahara, S. B. Lei, D. Mossinger, H. Kozuma, K. Inukai, M. V. der Auweraer, F. C. De Schryver, S. Hoger, Y. Tobe and S. De Feyter, *Chem. Commun.*, 2008, **33**, 3897-3899.
14. J. Lu, S. B. Lei, Q. D. Zeng, S. Z. Kang, C. Wang, L. J. Wan and C. L. Bai, *J. Phys. Chem. B*, 2004, **108**, 5161-5165.
15. Y. T. Shen, K. Deng, X. M. Zhang, W. Feng, Q. D. Zeng, C. Wang and J. R. Gong, *Nano Lett.*, 2011, **11**, 3245-3250.
16. X. Zhang, Y. Shen, S. Wang, Y. Guo, K. Deng, C. Wang and Q. Zeng, *Sci. Rep.*, 2012, **2**, 742.
17. Y. J. He, Q. Liu, W. Pan and X. W. Xiao, *Chemistry Online*, 2013, **76**, 517-521.
18. B. Delley, *J. Chem. Phys.*, 2000, **113**, 7756-7764.
19. J. P. Perdew and Y. Wang, *Phys. Rev. B*, 1992, **45**, 13244-13249.

## TOC



When dissolved in 1-phenyloctane, EDTTF could co-assemble with TCDB to form a hexagonal network and would transform into linear structure.